

# Chameleon2++: An Efficient Chameleon2 Clustering with Approximate Nearest Neighbors

Priyanshu Singh<sup>1</sup> and Kapil Ahuja<sup>2</sup>

<sup>1,2</sup>Math of Data Science & Simulation (MODSS) Lab, Computer Science and Engineering, Indian Institute of Technology Indore, 453552, Madhya Pradesh, India.

Contributing authors: [priyanshu250167@gmail.com](mailto:priyanshu250167@gmail.com); [kahuja@iiti.ac.in](mailto:kahuja@iiti.ac.in);

## Abstract

Clustering algorithms are fundamental tools in data analysis, with hierarchical methods being particularly valuable for their flexibility. Chameleon is a widely used hierarchical clustering algorithm that excels at identifying high-quality clusters of arbitrary shapes, sizes, and densities. Chameleon2 is the most recent variant that has demonstrated significant improvements, but suffers from critical failings and there are certain improvements that can be made.

The first failure we address is that the complexity of Chameleon2 is claimed to be  $O(n^2)$ , while we demonstrate that it is actually  $O(n^2 \log n)$ , with  $n$  being the number of data points. Furthermore, we suggest improvements to Chameleon2 that ensure that the complexity remains  $O(n^2)$  with minimal to no loss of performance. The second failing of Chameleon2 is that it lacks transparency and it does not provide the fine-tuned algorithm parameters used to obtain the claimed results. We meticulously provide all such parameter values to enhance replicability.

The improvement which we make in Chameleon2 is that we replace the exact  $k$ -NN search with an approximate  $k$ -NN search. This further reduces the algorithmic complexity down to  $O(n \log n)$  without any performance loss. Here, we primarily configure three approximate nearest neighbor search algorithms (Annoy, FLANN and NMSLIB) to align with the overarching Chameleon2 clustering framework. Experimental evaluations on standard benchmark datasets demonstrate that the proposed Chameleon2++ algorithm is more efficient, robust, and computationally optimal.

**Keywords:** Clustering Algorithm, Chameleon Clustering, Approximate Nearest Neighbors, Complexity Analysis

# 1 Introduction

Clustering in data mining is an unsupervised data analysis process that aims to group data points such that intra-cluster similarity is maximized while inter-cluster similarity is minimized (Xu and Tian 2015). This technique is critical in identifying meaningful patterns in large datasets. Among the various clustering algorithms, Chameleon (Karypis et al. 1999) (Ch1) is a popular hierarchical clustering algorithm that excels in identifying high-quality clusters or patterns of arbitrary shapes, sizes, and densities. Its dynamic modeling framework allows it to overcome the limitations of traditional algorithms that struggle with diverse cluster structures (Ezugwu et al. 2022).

Chameleon2 (Barton et al. 2019) (Ch2) is the most recent variant of this algorithm, which has shown to perform substantially better than all competing algorithms. This algorithm comprises of four main phases. First, Graph Generation, where an exact  $k$ -nearest-neighbor ( $k$ -NN) search is performed, followed by the construction of an exact  $k$ -NN tree. Second, Graph Partitioning, where algorithms such as Fiduccia-Mattheyse (FM) and the Hypergraph Multilevel Partitioning System (hMETIS) are applied. Although both methods are viable, FM is recommended for its slightly better performance over hMETIS. Third, a Partition Refinement algorithm called Flood-Fill, which addresses unbalanced partitions, that are often generated by the previous step while prioritizing minimal edge cuts. Fourth and lastly Graph Merging, which utilizes a dynamic model leveraging relative-interconnectivity and relative-closeness to identify clusters of arbitrary shapes with high quality.

In this work, we address the failings of Ch2, and also give its improvement. The *failings*, which we address are as follows:

- (a) First, the computational complexity of Ch2 when using FM for graph partitioning, as mentioned in the paper is  $O(n^2 + n + n \log m + m^2 \log m)$  where  $n$  is number of data points and  $m$  is number of partitions. The paper claims to bound the  $m$  by 100 making the overall complexity to be  $O(n^2)$ . We experimentally demonstrate that practically this  $m$  tends to  $n$  increasing the complexity to  $O(n^2 \log n)$ . Further, we recommend the use of hMETIS, which brings this cost to  $O(n^2)$ .
- (b) Second, Ch2 in its paper also mentions that to obtain the best performance fine tuning of algorithmic parameters is needed for each dataset, however, it does not provide the values of these parameters. We meticulously list these values, and demonstrate that the performance of our (local) implementation of Ch2 is the same as that of Ch2 from the original paper.

Next we describe the *improvement* made in the Ch2 algorithm. As stated in the original Ch2 paper, finding the exact  $k$  nearest neighbors is the most computationally expensive part of the algorithm (Barton et al. 2019). Here, we enhance Ch2 during the graph generation phase by replacing the exact  $k$ -NN search with an approximate  $k$ -NN search. We adapt three algorithms; Annoy, FLANN, and NMSLIB to achieve this. We retain the graph partitioning using hMETIS, flood-fill phase, and merging

criteria of Ch2. Thus, this improvement bounds the complexity of the overall algorithm by  $O(n \log n)$ . Experimentally, we demonstrate the corresponding time gain as well as the fact that use of approximate  $k$ -NN (instead of exact  $k$ -NN) incurs no loss in performance. We refer to our enhanced algorithm as Chameleon2++ (Ch2++).

The remainder of this paper has three main sections. In Section 2, we revisit the original Ch2 algorithm and address its two failings. Section 3 introduces Ch2++, which is an improvement to Ch2. Finally, in Section 4 we conclude with a summary of our findings and suggestions for future research.

## 2 Chameleon2: It’s Analysis and Experimentation

Here, in Section 2.1, we describe the standard Ch2 algorithm. In Section 2.2, we analyze the algorithm demonstrating that its existing complexity is higher than what is claimed, i.e.,  $O(n^2 \log n)$  instead of  $O(n^2)$ . Here, we also give a variant with a lower complexity. Finally, in Section 2.3, we give the experimental results where we provide the fine-tuned parameters that were missing in the original Ch2 paper.

### 2.1 The standard Chameleon2 algorithm

In this section, we present Ch2, a hierarchical agglomerative clustering algorithm. Ch2 operates in four key phases: graph generation, graph partitioning, partition refinement, and merging. The first two phases aim to partition the data into small subclusters, while the third refines these subclusters. Finally, the merging phase iteratively combines the subclusters to form the final clusters. These aspects are discussed in detail in the below subsections.

#### 2.1.1 Graph Generation

Transforming high-dimensional datasets into sparse graphs can effectively reveal underlying patterns in the data (Taunk et al. 2019). Here, this is achieved by using the  $k$ -Nearest Neighbor ( $k$ -NN) algorithm, which connects each node to its  $k$  most similar neighbors forming  $k$  edges per node. The edges are weighted based on the inverse of the distance between nodes, meaning shorter distances correspond to higher edge weights given by that  $\frac{1}{D(N1,N2)}$ .

Here,  $D$  is a distance function, usually Euclidean, and  $N1$  and  $N2$  are two nodes. In Ch2, a symmetrical  $k$ -NN graph is constructed, as it exhibits substantially fewer edges. Symmetrical  $k$ -NN constructs a graph in which an edge exists between two nodes only if *both* nodes belong to the  $k$ -nearest neighbors of each other. By eliminating redundant intra-cluster connections (focusing on more relevant relationships within the data), it improves clustering quality.

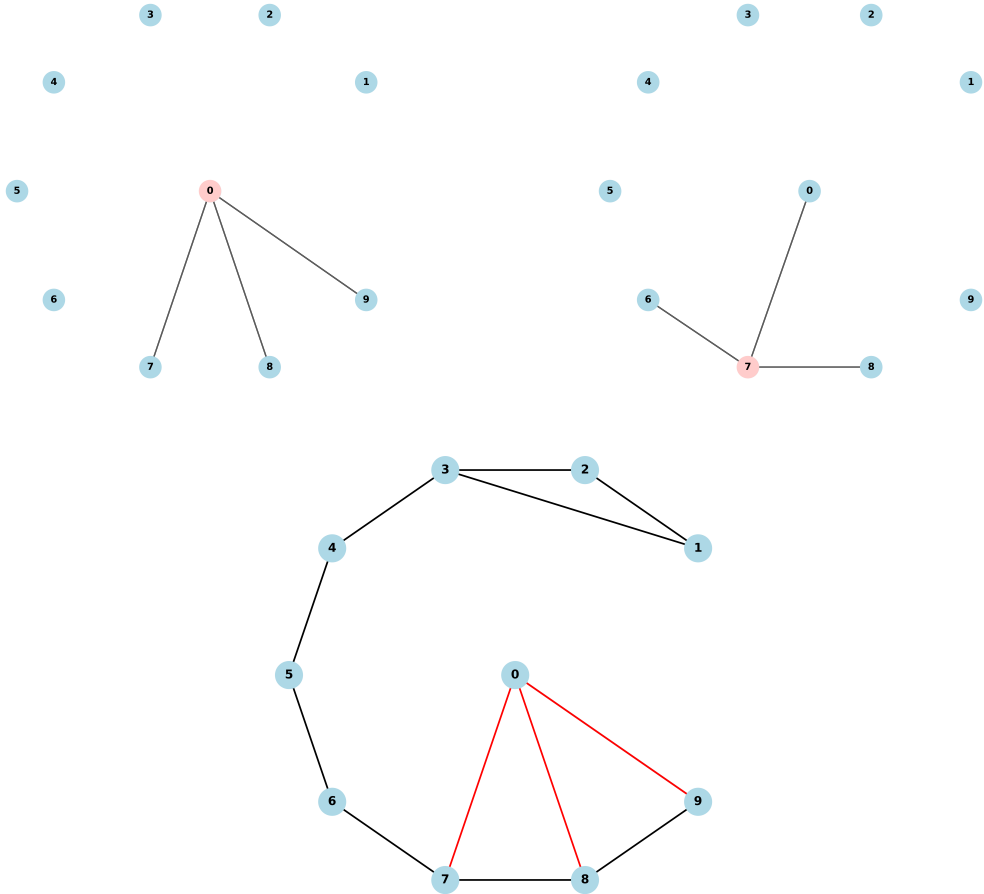


**Fig. 1** Visualization of 3-nearest neighbors: (Left) 3-NNs for node 0, (Right) 3-NNs for node 7, and (Bottom) Symmetrical 3-NNs graph.

Fig. 1 illustrates the construction of symmetrical  $k$ -NN graph for an abstract dataset, highlighting the intermediate step of identifying the  $k$ -NNs of two nodes and establishing edges only between mutual  $k$ -NNs in the final graph. Here, 0-7, 0-8, 0-9 have edges between them because they are in 3-NNs of each other. While 0-1, 0-2, 0-3, 0-4, 0-5, 0-6 do not have edges between them because although 0 is in 3-NNs of 1, 2, 4, 5, 6, vice-versa is not true (0 already has 7, 8, 9 as symmetrical 3-NNs).

The graph generation algorithm uses exact  $k$ -nearest neighbors and has a run-time complexity of  $O(n^2)$ , where  $n$  denotes the number of nodes in the graph (or dataset).

### 2.1.2 Graph Partitioning

This section explores two prominent graph partitioning algorithms which primarily take a  $k$ -NN graph as an input (in-terms of Chameleon clustering). We first summarize

the Fiduccia-Mattheyses (FM) algorithm as utilized in Ch2. Then we introduce the Hypergraph-based Multi-level Recursive Bisection (hMETIS) algorithm, which is also introduced in Ch2 but not recommended.

The goal of graph partitioning is to divide a graph into multiple subclusters of roughly equal size while minimizing the edge-cut, i.e., the total number of edges (or weights) connecting nodes between different subclusters. Both algorithms employ recursive bisection, iteratively splitting the graph into halves until reaching the desired number of partitions or a specified size threshold.

### *Fiduccia-Mattheyses Algorithm*

FM is a variant of the Kernighan-Lin (KL) algorithm (Kernighan and Lin 1970), which we discuss below. Initially, the algorithm generates a random partition of the input graph, dividing it into two approximately equal-sized parts. Then, it computes the gain for each node, referred to as potential change in minimum cut-size if the node was moved to the opposite partition. These gains are stored in a data structure called a gain-bucket.

Fig. 2 illustrates an example with 4 nodes connected by certain edges, with a random red-colored cut showing the initial partition. The left side of the figure is the initial iteration, while the right side depicts the final iteration, marking the completion of the first pass. While looking at the left figure, on the left side of the partition, moving node  $v_2$  would reduce the cut size by 2, as shown in the left figure (hence, its gain is  $+2$ ), while moving node  $v_0$  to other side would result in a gain of  $+1$ . We can similarly compute the gains on the right side of the partition.

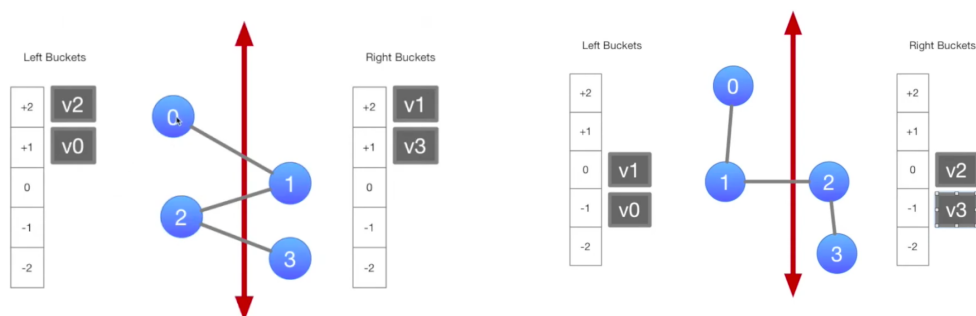


**Fig. 2** FM utilizing gain bucket data structure to select the optimal cut and update buckets for the next pass. (Left) Initial bucket values for each node. (Right) Bucket updates after a single pass.

Next, the algorithm iteratively selects the node with the highest gain from each partition and moves it to the other partition. After each move, the selected node is locked and excluded from future iterations, while the gains of its neighboring nodes are updated in the gain bucket. The algorithm continues selecting and moving nodes from the remaining unlocked set. Upon completing all node moves, the configuration with the smallest cut-size observed during the process is chosen as the final partition.

This completes one pass of the algorithm. The result of one complete pass is depicted in right side of Fig. 2.

Once the first pass is completed, then the configuration of the smallest cut-size becomes the starting point of performing another pass on it. These multiple passes are performed because the nature of the algorithm is greedy and it may result in the algorithm getting stuck in a local minima. This continues until no further improvement is achieved or a maximum number of passes is reached. The Ch2 algorithm does not use the standard FM algorithm; instead, it employs a recursive version known as recursive FM bisection. The algorithm utilized in Ch2 requires one parameter,  $p_{max}$ , defining the maximum number of nodes in a single partition (stopping criteria). The FM bisection is repeated on each resulting partition until all clusters contain no more than  $p_{max}$  nodes. The time complexity of the algorithm is  $O(n + n \log m)$ , where  $n$  is the number of nodes in the graph and  $m$  denotes number of partitions bounded by  $p_{max}$ .

### ***hMETIS***

hMETIS, developed in (Karypis et al. 1997), is a multilevel partitioning algorithm designed for hypergraphs where edges can connect more than two nodes, as shown in Fig. 3. In comparison, the FM algorithm operates on traditional graphs.

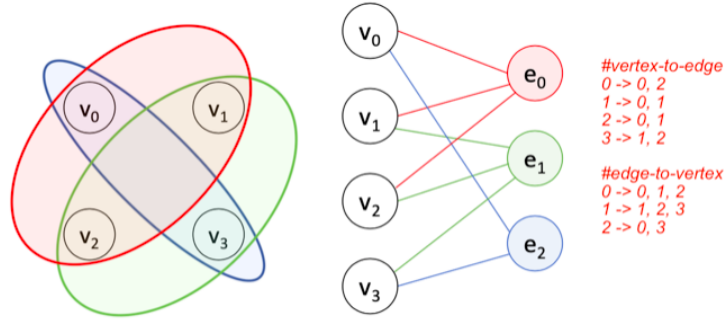


**Fig. 3** The figure on the left illustrates a hypergraph, while the figure on the right depicts its equivalent bipartite representation.

The hMETIS algorithm consists of three key phases: coarsening, initial partitioning, and uncoarsening (refinement) (Schlag et al. 2023), as illustrated in the Fig. 4.

1. **Coarsening Phase** - In this phase, hMETIS iteratively creates a sequence of smaller hypergraphs by collapsing nodes and hyperedges. The algorithm uses various matching schemes to identify sets of nodes to be combined, such as edge coarsening, hyperedge coarsening, or modified hyperedge coarsening (Karypis and Kumar 1998). For example, it combines the nodes which have large number of edges

between them. This process continues until the hypergraph is sufficiently small for initial partitioning.

2. **Initial Partitioning Phase** - Once the hypergraph is coarsened to a manageable size, hMETIS applies a simple partitioning algorithm (such as KL) to create an initial partition. This step is crucial as it provides a starting point for the subsequent refinement process.
3. **Uncoarsening and Refinement Phase** - In this phase, hMETIS gradually expands the partitioned hypergraph back to its original size. At each level of uncoarsening, the algorithm applies refinement techniques to improve the partition quality. The refinement process in hMETIS is similar to FM, but with important distinctions to handle hyperedges such as below.
  - The gain calculation for moving a node considers all hyperedges it belongs to, not just binary edges.
  - The gain bucket structure requires modification to accommodate hyperedge gain updates. Unlike FM's single-array approach, the data structure implementation necessitates multiple arrays to efficiently manage gain calculations.
  - The algorithm may also perform multiple iterations, allowing moves that temporarily increase the cut size to escape local optima.

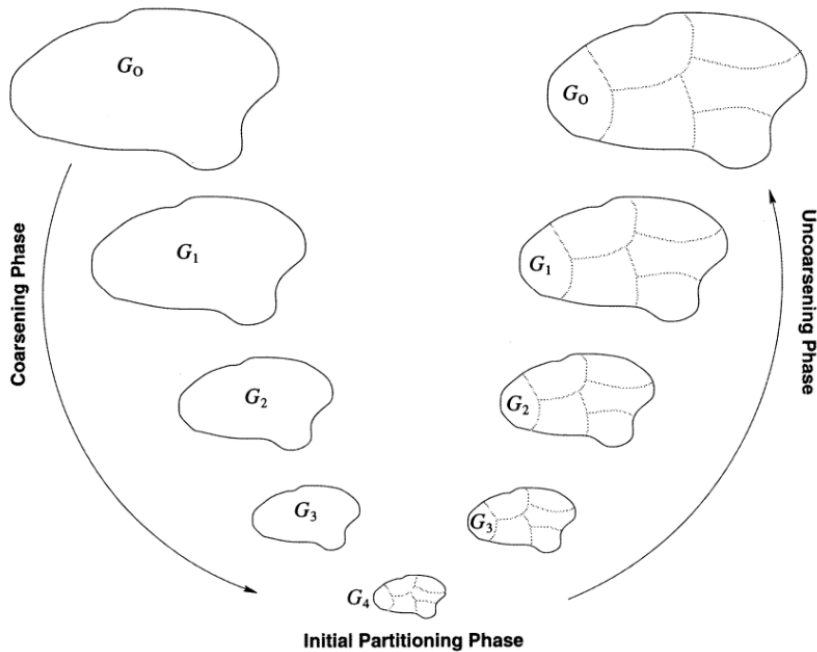


**Fig. 4** The various phases of hMETIS at a glance, a multilevel partitioning algorithm.

hMETIS additionally employs several optimization techniques such as V-cycle Refinement, Adaptive Coarsening and Balancing Constraints etc. ([Karypis and Kumar](#)

1999), to improve both the quality of partitions and the algorithm’s runtime. hMETIS has a runtime complexity of  $O(n + m \log m)$ , where  $n$  denotes the number of nodes in the hypergraph and  $m$  is the number of final partitions desired, ideally ( $m \ll n$ ). Although in recursive FM bisection Ch2 provides a bound on  $m$ , but here they don’t.

### 2.1.3 Flood-Fill

A major issue with partitioning algorithms is their tendency to create disconnected partitions while minimizing edge cuts. These widely separated partitions lack internal connectivity, which cannot be corrected in later stages, resulting in incorrect merges during the merging phase and ultimately degrading overall clustering quality. Fig 5 illustrates this issue. Here, to achieve a minimal edge cut, the graph is partitioned into disconnected partitions (excluded by red-borders).

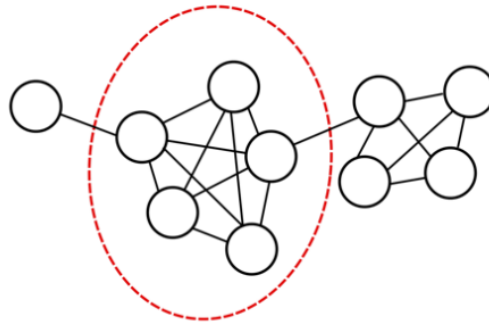


**Fig. 5** The red border separates the connected partition (within the border) and disconnected partition (outside the border).

To address this issue, Ch2 employed a local breadth-first search (BFS) based heuristic called Flood-Fill on the partitioned  $k$ -NN graph, which detects the disconnected components within the partitions. If a partition consists of multiple disconnected components, the algorithm separates them into disjoint connected partitions. This approach ensures that partitions are cohesive and do not contain disjoint substructures. By this approach, Ch2 achieves significantly better clustering quality effectively. Here, the run-time complexity of the heuristic is  $O(n)$ .

### 2.1.4 Merging

This section outlines the final phase of the algorithm, known as the merging phase. After partitioning and flood-fill, several small sub-clusters are generated, which must be merged to form the final clusters. To achieve this most existing algorithms rely just on external properties. For example, the distance between the centers of the clusters, etc. (Saxena et al. 2017). However, besides external properties, the internal properties of clusters plays a crucial role to achieve better clustering, for example



density of the clusters.

Here, merging in Ch2 draws primary inspiration from (Karypis et al. 1999) and (Shatovska et al. 2012) and is performed using two similarity metrics, one is Relative-Interconnectivity ( $R_{IC}$ ), and the other one is Relative-Closeness ( $R_{CL}$ ). Abstractly,  $R_{IC}$  favors merging of clusters that are far apart but are well connected, on the contrary  $R_{CL}$  is a dual of  $R_{IC}$  favoring merging of clusters that are spatially close but are not well connected. Next, we define the mathematical formulation of these. If  $C_i$  and  $C_j$  denote  $i$ th and  $j$ th clusters, then the  $R_{IC}$  between them is defined as follows (Barton et al. 2019):

$$R_{IC}(C_i, C_j) = \begin{cases} 1, & \text{for } |E_{C_i}| \vee |E_{C_j}| = 0, \\ \frac{|E_{C_{i,j}}|}{\min\{|E_{C_i}|, |E_{C_j}|\}} \cdot \rho(C_i, C_j)^\beta & \text{for } |E_{C_i}| \wedge |E_{C_j}| > 0. \end{cases} \quad (1)$$

Above, first row signifies singleton clusters and second row takes care of all the other cases. Here,  $|E_{C_{i,j}}|$  represents the number of edges between cluster  $C_i$  and  $C_j$ ;  $|E_{C_i}|$  denotes the number of edges within cluster  $C_i$ ; and  $|E_{C_j}|$  denotes the number of edges within cluster  $C_j$ . Finally,  $\rho$  discourages the algorithm from merging clusters with different densities and the  $\beta$  parameter (with default value of 1.0) serves to modify the weight of the  $\rho$  factor. The expression for  $\rho$  is given as below (Shatovska et al. 2012).

$$\rho(C_i, C_j) = \frac{\min\{\bar{s}(C_i), \bar{s}(C_j)\}}{\max\{\bar{s}(C_i), \bar{s}(C_j)\}}, \quad (2)$$

where,

$$\bar{s}(C_i) = \frac{1}{|E_{C_i}|} \sum_{e \in C_i} w(e). \quad (3)$$

Here,  $w(e)$  denotes the weight of an edge  $e$  within a cluster  $C_i$ . Similarly, the formula for Relative-Closeness ( $R_{CL}$ ) is given as follows:

$$R_{CL}(C_i, C_j) = \begin{cases} m_{fact} \cdot \frac{\bar{s}(C_i, C_j)}{s(C_i) + s(C_j)} & \text{for } |E_{C_i}| \vee |E_{C_j}| = 0, \\ (|E_{C_i}| + |E_{C_j}|) \cdot \frac{\bar{s}(C_i, C_j)}{s(C_i) + s(C_j)} & \text{for } |E_{C_i}| \wedge |E_{C_j}| > 0. \end{cases} \quad (4)$$

Here, as above, the first line captures the singleton case and the second captures all the other cases. Here,  $m_{fact}$  is a constant factor which ensures that singleton clusters obtain higher similarity value, which causes them to merge with their neighbors in the early stages of the merging process.

Finally, at each iteration, Ch2 selects the cluster pairs which maximize  $S_{Ch2}$  given below. This is done until  $(c)$  clusters, i.e., the final number of clusters are left.

$$S_{Ch2}(C_i, C_j) = R_{CL}(C_i, C_j)^\alpha \cdot R_{IC}(C_i, C_j), \quad (5)$$

where,  $\alpha$  is a user-defined parameter with default value of 2.0 respectively.

The naive merging process would have complexity of  $O(m^3)$ . By using a priority queue, we can reduce this complexity to  $O(m^2 \log m)$  with  $(m)$  merging steps.

Algorithm	Graph Generation	Graph Partitioning	Partition Refinement	Merging
Ch2	exact Symm. $k$ -NN	Recursive FM Bisection	Flood-Fill	$R_{CL}^\alpha * R_{IC}$
Complexity	$O(n^2)$	$O(n + n \log m)$	$O(n)$	$O(m^2 \log m)$

**Table 1** Ch2 at a glance.

The final complexity of Ch2 is summarized in the table above, i.e.,  $O(n^2 + n + n \log m + n + m^2 \log m)$ . Additionally, Ch2 claims that  $m$  is significantly smaller than  $n$ , (i.e.,  $m \ll n$ ), and therefore, the overall complexity is generally  $O(n^2)$ .

## 2.2 Analysis: Addressing the First Failing of Ch2

In general, hMETIS has the following advantages over the FM algorithm:

- hMETIS is generally faster and robust than the repeated applications of FM for large problem instances.
- It can handle hypergraphs directly, making it more suitable to find high-quality partitions more consistently for problems that naturally involve multi-way relationships.

In the current set of experiments, which are based on the experiments conducted by Ch2, the two advantages of hMETIS do not apply. This is because we are neither working with very large datasets nor are we dealing with hypergraphs. Hence, if FM gives higher accuracy or clustering quality then it should be preferred, which the Ch2 paper does. However, an important aspect overlooked in the Ch2 paper is the complexity of the merging phase, which depends on the number of partitions ( $m$ ).

The bound for  $m$ , as given by  $p_{max}$ , for recursive FM bisection under Ch2 is taken as  $\max(5, n/100)$ , where  $n$  is the number of nodes. Since for hMETIS the Ch2 paper does not provide any bound on  $m$ , we propose  $2 \log n$  based upon our experimental intuition. In general, the  $m$  need to be larger than the number of final clusters ( $c$ ) so that merging could be performed. In cases when  $2 \log n$  turns out to be less than  $c$ , merging cannot be done. Hence, to prevent this scenario we bound  $m$  by  $2c$ . Thus, the overall bound of  $m$  is taken as  $\max(2 \log n, 2c)$ .

In Table Fig. 2, we present the number of partitions obtained using the FM algorithm and the hMETIS algorithm on a benchmark dataset named *compound*, both before the flood-fill phase and after it. We observe that before the flood-fill phase, the FM algorithm produces the number of partitions ( $m$ ) substantially smaller than the number of nodes ( $n$ ) (i.e.,  $m \ll n$ ), while post-flood-fill, the number of partitions approaches  $n$  (i.e.,  $m \approx n$ ). In contrast, the hMETIS algorithm generates the number of partitions significantly smaller than the number of nodes both before and after the flood-fill phase (i.e.,  $m \ll n$ ). We generalize this observation by conducting

experiments on all the standard benchmark datasets used in Ch2, which is discussed next.

Partitioning Algorithm	No. of partitions ( $m$ )	
	Before Flood-Fill	After Flood-Fill
Recursive FM Bisection	103	354
hMETIS	16	20

**Table 2** No. of partitions ( $m$ ) given ( $n=399$ ) for compound dataset.

Next, we analyze the number of partitions on all the standard benchmark datasets when using FM and hMETIS. The results before flood-fill are presented in Fig. 6. As evident, in both FM and hMETIS,  $m$  is significantly smaller than  $n$  (i.e.,  $m \ll n$ ). The results after flood-fill are presented in Fig. 7. As evident, in FM  $m$  approaches nearly  $n$  (i.e.,  $m \approx n$ ), while in hMETIS  $m$  still remains significantly smaller than  $n$  (i.e.,  $m \ll n$ ). Consequently, the merging complexity of FM increases to  $O(n^2 \log n)$ , while for hMETIS it remains  $O(m^2 \log m)$ .

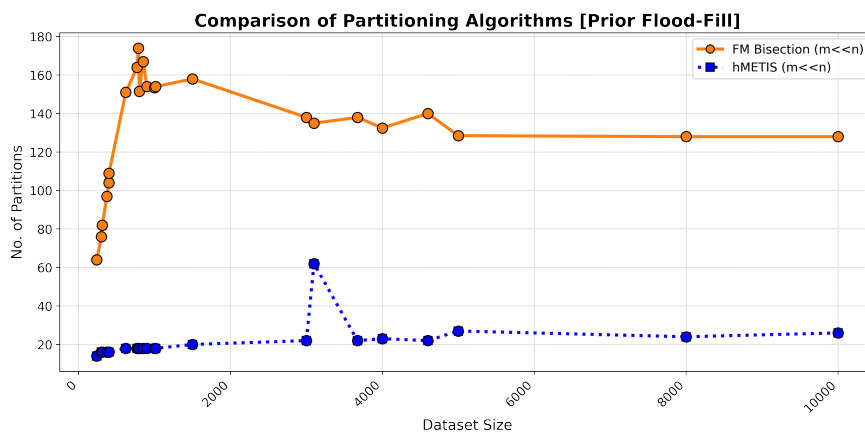


**Fig. 6** No. of partitions at the end of graph partitioning phase.

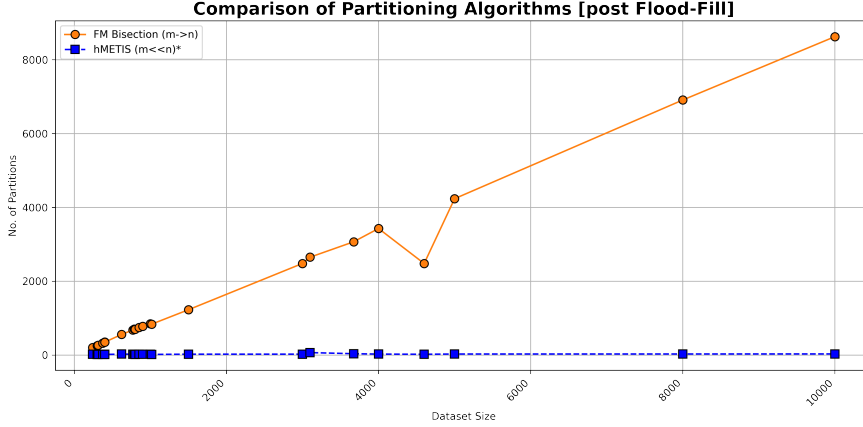


Fig. 7 No. of partitions at the end of flood-fill phase.

As shown in Table 2, the overall complexity of FM-based Ch2 reaches  $O(n^2 \log n)$ , while that of hMETIS-based Ch2 remains  $O(n^2)$ .

Algorithm	Graph Generation	Graph Partitioning	Flood-Fill	Merging	Complexity
Ch2 - FM	$O(n^2)$	$O(n + n \log m)$	$O(n)$	$O(n^2 \log n)$	$O(n^2 \log n)$
Ch2 - hMETIS	$O(n^2)$	$O(n + m \log m)$	$O(n)$	$O(m^2 \log m)$	$O(n^2)$

Table 3 FM vs hMETIS at a glance.

## 2.3 Experiments: Addressing the Second Failing of Ch2

Here, we have three sections, Section 2.3.1 discusses the setup, Section 2.3.2 gives the insights on the parametric configuration, and Section 2.3.3 compares the original Ch2 results with the newly obtained ones.

### 2.3.1 Setup

Here, we initially describe the standard benchmark datasets as experimented in the Ch2 paper. Further we discuss the evaluation metric, again as used in the Ch2 paper.

#### Dataset

Detailed specifications of the benchmark datasets are provided in Table 4, where dimensions ( $d$ ), dataset size ( $n$ ), noise (%), and the final number of clusters (classes) are outlined for each dataset. These datasets are taken from <sup>1</sup>github. Each dataset here presents human-distinguishable structures, providing a challenging yet controlled environment for evaluating the algorithm’s performance.

<sup>1</sup><https://github.com/deric/clustering-benchmark>

Dataset	$d$	$n$	noise (%)	classes
3-spiral	2	312	-	3
aggregation	2	788	-	7
atom	3	800	-	2
chainlink	3	1,000	-	2
cluto-t4-8k	2	8,000	764 (9.55%)	7
cluto-t5-8k	2	8,000	1153 (14.41%)	7
cluto-t7-10k	2	10,000	792 (9.92%)	10
cluto-t8-8k	2	8,000	323 (4.04%)	9
compound	2	399	-	6
cure-t2-4k	2	4,000	200 (4.76%)	7
D31	2	3,100	-	31
dense-disk-5k	2	5,000	-	2
diamond9	2	3,000	-	9
disk-in-disk	2	4,600	-	2
dpb	2	4,000	657 (16.43%)	6
DS-850	2	850	-	5
flame	2	240	-	2
impossible	2	3,673	78 (2.12%)	8
jain	2	373	-	2
long1	2	1,000	-	2
longsquare	2	900	-	6
lsun	2	400	-	3
pathbased	2	300	-	3
s-set1	2	5,000	-	15
sizes1	2	1,000	-	4
smile1	2	1,000	-	4
spiralsquare	2	1,500	-	6
target	2	770	-	6
triangle1	2	1,000	-	4
twodiamonds	2	800	-	2
wingnut	2	1,016	-	2
zelnik4	2	622	138 (22.19%)	5

**Table 4** Standard benchmark datasets from Ch2.

### *Evaluation Metric*

This study employs Normalized Mutual Information (NMI) (Shannon 1948) as the primary evaluation metric. Here, NMI is preferred because we have labeled datasets available, allowing for a normalized and symmetric comparison between the clusters and the existing ground truth labels. Further, NMI remains relatively insensitive to variations in cluster sizes. The formula for it is expressed as:

$$\text{NMI} = \frac{2 \times I(X; Y)}{H(X) + H(Y)}. \quad (6)$$

Here,  $I(X; Y)$  represents the mutual information between the true labels  $X$  and the predicted labels  $Y$ , while  $H(X)$  and  $H(Y)$  denote the entropy of the true and predicted labels, respectively. NMI ranges from 0 to 1, with higher values indicating greater agreement between the clustering solution and the ground truth labels. It effectively captures both the completeness and homogeneity of the clusters.

### 2.3.2 Parametric Configuration Insights

In this section, we give the parameter values for hMETIS Ch2 on the standard benchmark datasets. These values are categorized as default and fine-tuned for some particular datasets. The default values are given in Table 5 that matches those in the Ch2 paper. The fine-tuned values are given in Table 6 that were not reported in the Ch2 paper, and hence are new.

Algorithm	Parameter	Description	Default Value
Chameleon2	$k$	no. of neighbors ( $k$ -NN)	$2 \ln(n)$
	$p_{max}$	max partition size	$\max\{5, n/100\}$
	$m_{fact}$	factor for small clusters	$10^3$
	$\alpha$	closeness	2.0
	$\beta$	interconnectivity	1.0

Table 5 Default parameter values for Ch2.

Dataset	$k$	$m$	$\alpha$	$m_{fact}$
3-spiral	$\ln n$	-	-	-
aggregation	-	-	-	-
atom	-	-	-	-
chainlink	-	-	-	-
cluto-t4.8k	-	-	-	-
cluto-t5.8k	$3 \log 2n$	-	4	-
cluto-t7.10k	$3 \log 2n + 2$	-	2	-
cluto-t8.8k	$3 \log 2n$	-	2	-
compound	$2 \ln n$	-	-	-
cure-t2-4k	$\ln n$	-	-	-
D31	-	-	-	-
dense-disk-5k	$3 \log 2n + 2$	-	1	-
diamond9	$\log 2n$	-	-	-
disk-in-disk	-	-	2	-
dpb	$\log 2n$	-	-	-
DS-850	-	-	-	-
flame	$\log 2n + 2$	-	-	-
impossible	$\ln n + 2$	-	2	-
jain	$2 \ln n$	-	-	-
long1	-	-	-	-
longsquare	-	-	-	-
lsun	$2 \ln n$	-	-	-
pathbased	-	-	-	-
s-set1	-	-	-	-
sizes1	$\log 2n$	-	-	-
smile1	-	-	-	-
spiralsquare	-	-	-	-
target	$2 \ln n$	-	-	-
triangle1	-	-	-	-
twodiamonds	-	-	-	-
wingnut	-	-	-	-
zelnik4	-	-	-	-

Table 6 Fine-tuned parameter values for Ch2.

### 2.3.3 Original v/s New Experimental Results

In Table 7, we present the NMI values obtained using different graph partitioning algorithms. Here, Column 1 lists the dataset names, while Columns 2 and 3 provide the NMI values for hMETIS Ch2 from the original paper and our local implementation, respectively. Column 4 reports the NMI values for recursive FM Ch2 from the original study.

Dataset	hMETIS		FM
	Paper	Local	
3-spiral	<b>1.00</b>	<b>1.00</b>	<b>1.00</b>
aggregation	0.97	0.97	<b>0.99</b>
atom	<b>1.00</b>	<b>1.00</b>	<b>1.00</b>
chainlink	<b>1.00</b>	<b>1.00</b>	<b>1.00</b>
cluto-t4.8k	0.87	0.82	<b>0.89</b>
cluto-t5.8k	0.82	0.83	<b>0.86</b>
cluto-t7.10k	0.87	0.77	<b>0.91</b>
cluto-t8.8k	<b>0.94</b>	0.90	<b>0.94</b>
compound	0.91	0.98	<b>0.99</b>
cure-t2-4k	0.90	0.92	<b>0.97</b>
D31	<b>0.96</b>	0.95	<b>0.96</b>
dense-disk-5k	0.78	0.82	<b>0.91</b>
diamond9	<b>1.00</b>	<b>1.00</b>	0.99
disk-in-disk	0.79	0.75	<b>0.99</b>
dpb	0.78	0.72	<b>0.81</b>
DS-850	<b>0.99</b>	<b>0.99</b>	0.98
flame	<b>0.96</b>	0.93	0.93
impossible	0.96	0.91	<b>0.97</b>
jain	<b>1.00</b>	<b>1.00</b>	<b>1.00</b>
long1	<b>1.00</b>	<b>1.00</b>	<b>1.00</b>
longsquare	0.97	<b>1.00</b>	0.98
lsun	<b>1.00</b>	<b>1.00</b>	<b>1.00</b>
pathbased	<b>0.92</b>	0.88	0.89
s-set1	0.98	0.98	<b>1.00</b>
sizes1	0.90	0.89	<b>0.91</b>
smile1	<b>1.00</b>	<b>1.00</b>	<b>1.00</b>
spiralsquare	0.95	0.97	<b>0.99</b>
target	0.94	<b>1.00</b>	<b>1.00</b>
triangle1	<b>1.00</b>	<b>1.00</b>	<b>1.00</b>
twodiamonds	<b>1.00</b>	<b>1.00</b>	<b>1.00</b>
wingnut	<b>1.00</b>	<b>1.00</b>	<b>1.00</b>
zelnik4	0.94	<b>0.99</b>	<b>0.99</b>
AVG. ( $\mu$ )	0.94	0.94	0.96
SD. ( $\sigma$ )	0.07	0.08	0.05

**Table 7** NMI values for clustering results generated by Ch2 using hMETIS and FM algorithms, respectively.

Two primary insights emerge from this comparison. First, the NMI values for our hMETIS Ch2 closely align with those reported in the original paper, thus validating our implementation. Second, as anticipated, hMETIS Ch2 demonstrates a slightly lower average NMI value than FM, with a difference of approximately 2%. Despite this, hMETIS remains preferable due to its reduced computational complexity of  $O(n^2)$ , as compared to FM’s  $O(n^2 \log n)$ , where  $n$  is the dataset size.

### 3 Chameleon2++: Proposed Algorithm and Results

Here, in Section 3.1 we first introduce our proposed Chameleon2++ algorithm i.e., the improved variant of Ch2 algorithm. Next, in Section 3.2 we showcase our experimental results obtained on Ch2++.

#### 3.1 Proposed Chameleon2++ Algorithm

In this section, we describe our Ch2++ algorithm including its phases of graph generation, graph partitioning, flood-fill and merging, in the respective subsections below.

##### 3.1.1 Graph Generation: Approximate $k$ -NN Graph

As discussed before, for traditional exact  $k$ -NN graphs, an exhaustive search is conducted to find the  $k$ -nearest neighbors of a data item by evaluating its euclidean distance with all remaining data items, spanning the entire search space. In contrast, the approximate  $k$ -NN graph utilizes approximate nearest neighbor search (ANNS) techniques, which reduce the search space by eliminating irrelevant data items. The objective is to limit computation to a select subset of data points, particularly those in close proximity to the target item (Abbasifard et al. 2014), thereby improving efficiency at the cost of potentially missing some data points.

Here, in Ch2++, we utilize and generate a symmetrical approximate  $k$ -NN graph using ANN search based algorithms such as Annoy, FLANN, and NMSLIB (Li et al. 2019). There are many different variants of these algorithms available in (Aumüller et al. 2020), (Malkov et al. 2014), however, selecting the most suitable one for our overall design and integrating it posed a significant challenge. We discuss them below.

##### *Annoy (Approximate Nearest Neighbors Oh Yeah)*

Annoy is one of the simple and effective algorithm in the category of approximate nearest neighbors search (Li et al. 2019).



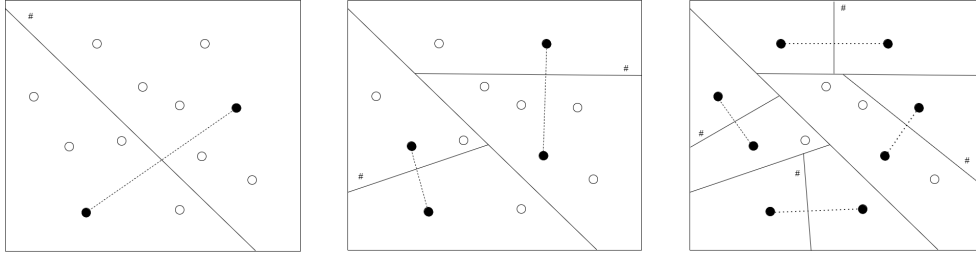


**Fig. 8** Initial recursive bi-partitioning of search-space in Annoy.

Initially, two random data points are selected, and a binary spaced partitioning is performed based on a selected hyperplane. The hyperplane here is defined as the perpendicular bisector of the line segment connecting the two selected data points. This process is recursively performed, where the data points are chosen from the subset of data being partitioned at each step. This process continues until each partition has  $\leq k$  items (here,  $k$  is leaf-size parameter). This process is illustrated in Fig. 8.

Next, a Random Projection tree (RP-tree) is built, which serves as the indexing mechanism for nearest neighbor queries. The internal nodes here represent the hyperplane and the leaf-nodes denote the search subspace. Let  $q$  be the query data point for which the  $k$ -nearest neighbors are required. Starting with the root of a tree, the path to that child of the root is traversed which is closer to  $q$ . This process is repeated until we reach a leaf node. The leaf node gives the  $k$ -nearest neighbors for  $q$ . Building of a sample RP-Tree is shown in Fig. 9. Here, the number inside the node denotes the count of data points present in that subspace.

When we perform the initial recursive bi-partitioning of the search space, points are chosen at random. To improve the accuracy and search performance of the algorithm this partitioning is performed in-parallel, with different sets of initial random points, and subsequently multiple RP trees are built. The search is then conducted simultaneously across all trees using a priority queue-based traversal. Finally, the union of all the data points obtained from the leaf nodes of all the trees are taken into consideration (after removing duplicates). This gives us the final search subspace for the  $k$ -nearest neighbors for  $q$ .

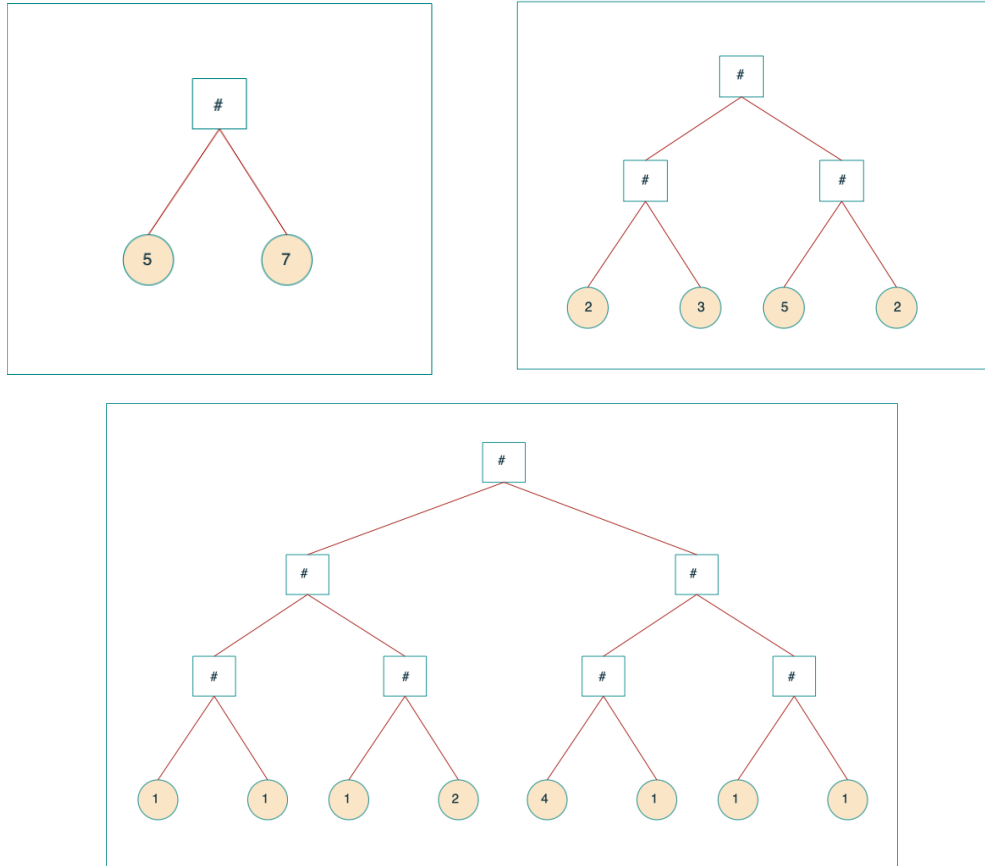


**Fig. 9** Building the tree-based index for searching in Annoy.

The time complexity for index construction in Annoy is  $O(n \log n)$ , where  $n$  is the number of points in the dataset. For searching, the time complexity is  $O(n^p \log n)$ , where  $p < 1$ , typically around 0.5, making it sublinear in practice.

***FLANN (Fast Library for Approximate Nearest Neighbors)***

FLANN is an ANN search algorithm designed for fast approximate nearest neighbor searches in high-dimensional spaces. It uses different tree-based algorithms such as randomized  $kd$ -tree, priority search  $k$ -means tree, and linear scan. As stated in (Li et al. 2019), (Dasgupta and Freund 2008), the randomized  $kd$ -tree performs effectively across most situations and hence, we use it.

Here, given a  $d$ -dimensional dataset, the top  $N_d$  dimensions with the highest variance are selected. A random splitting dimension is then chosen from these top  $N_d$  dimensions, and the data points are divided into two halves using a perpendicular hyperplane centered on the median value of the selected dimension (Otair 2013).

Subsequently, the data points are further split based on the remaining unused top  $N_d$  dimensions. This process continues iteratively until all top  $N_d$  dimensions are exhausted. The entire procedure is then recursively repeated.

This process for a 2 dimensional data is shown in Fig. 10, where the splitting dimension oscillates between the chosen  $N_d$  dimensions at each level. First, the data is split along the  $x$ -dimension, then along the  $y$ -dimension, and then again along the  $x$ -dimension, until either the number of points in a node fall below a specified leaf-size threshold or the maximum tree depth is reached.

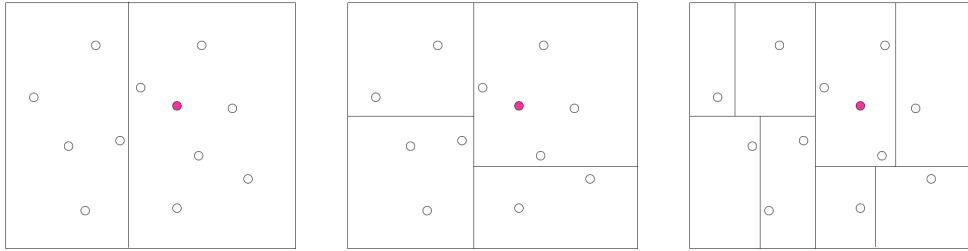


**Fig. 10** Recursive partitioning splits for a 2D dataset in FLANN.

The  $k$ -d tree is built with the internal nodes representing the splitting dimension (along with the median value), and leaf node signifying the actual data-points (final subspace). The searching in the tree is similar to as in Annoy. An example  $kd$ -tree is shown in Fig. 11 with splitting dimension underlined as well as mentioned on right.

Since the splitting is done randomly, this process is repeated for multiple splittings for which multiple  $kd$ -trees are built. Similarly, while querying a data point ( $d$ ), a priority queue-based depth-first search is conducted across all trees simultaneously. The search uses a heuristic scoring function that favors child nodes closer to the query point. The algorithm maintains a single priority queue for all trees and a shared candidate result set.

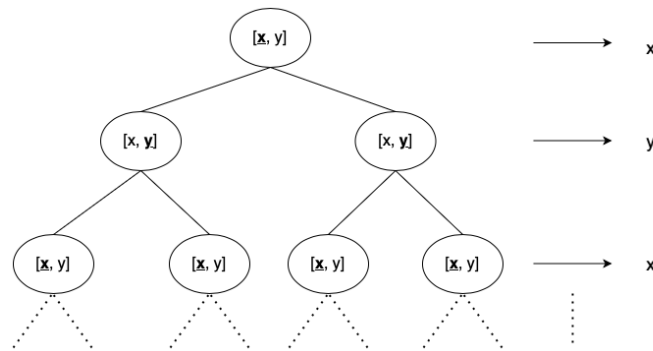


**Fig. 11** A  $kd$ -tree in FLANN.

The time complexity for the index construction in FLANN is  $O(n \log n)$ , where  $n$  is the number of points in the dataset. For searching, the time complexity is  $O(\log n)$  on average, but can degrade to  $O(n)$  in the worst case. In practice, FLANN’s performance is often sublinear, with search times typically scaling as  $O(n^p)$ , where  $p < 1$ , depending on the dataset characteristics and algorithm parameters.

***NMSLIB (Non-Metric Space Library)***

The Non-Metric Space Library (NMSLIB) implements the Hierarchical Navigable Small World (HNSW) algorithm (Malkov and Yashunin 2018) for efficient approximate  $k$ -nearest neighbor search. The algorithm’s fundamental principle mirrors the “six degrees of separation” concept, which suggests that any two people in the world are connected through at most six social connections. At the heart of HNSW is a hierarchical layered graph structure.

Each node (representing a data point) in the graph is assigned a random level  $l$  that determines its maximum layer participation. For instance, if a node is assigned  $l = 2$ , it appears in layers 0, 1, and 2. The level assignment follows a geometric distribution, resulting in most nodes having  $l = 0$ . At each layer, nodes maintain connections to at most  $M$  nearest neighbors, where  $M$  is a user-defined parameter. The resulting multi-layer structure is illustrated in Fig. 12.

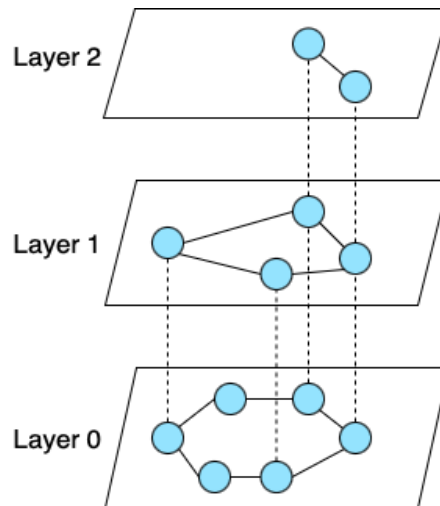


**Fig. 12** A sample HNSW graph.

The  $k$ -nearest neighbor search process begins at a randomly selected entry point in the topmost layer. At each layer, the algorithm performs a greedy search; it examines the current node’s neighbors and moves to the neighbor closest to the query point. This neighbor then serves as the entry point for the search in the layer below. This process repeats until reaching the bottom layer (layer 0), where a more thorough local search

is performed to find the  $k$ -nearest neighbors of the query point. Fig. 13 illustrates this search procedure.

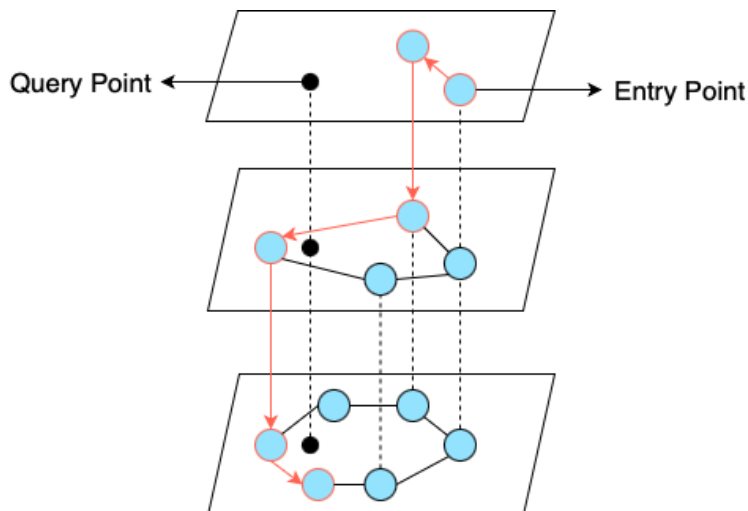


**Fig. 13** Searching the HNSW graph.

The time complexity for index construction is  $O(n \log n)$ , where  $n$  is the number of data points, while search complexity is approximately  $O(\log n)$  for datasets with low intrinsic dimensionality.

#### **Conclusion:**

Traditional exact  $k$ -nearest neighbor computation requires  $O(n)$  time to find the  $k$ -nearest neighbors of a data item, resulting in an overall complexity of  $O(n^2)$  for dataset with  $n$  items. However, by utilizing ANN search techniques, we significantly mitigate this complexity to  $O(n \log n)$ , enabling more efficient and scalable computations.

### **3.1.2 Graph Partitioning**

As discussed in the previous section, we have integrated hMETIS in Ch2. We use the same implementation here, i.e., the parameter  $m$ , is selected as  $m = \max(2 \log n, 2c)$ , where  $m$  defines the number of partitions, and  $c$  denotes the final number of clusters desired by the user. Here, the complexity stands out to be  $O(n + m \log m)$ , where  $n$  is the number of nodes.

### **3.1.3 Flood-Fill**

Here again, we use the flood-fill from Ch2 as depicted in the previous section, whose computational complexity is  $O(n)$  given  $n$  as the datasize.

### 3.1.4 Merging

Here again, we use the merging criteria from Ch2 as illustrated in the previous section. The time complexity for which turns out to be  $O(m^2 \log m)$ , where  $m$  denotes number of partitions obtained after flood-fill.

Finally, the Ch2++ base similarity combines both relative interconnectivity and relative closeness, similar to Ch2. Hence, at each iteration Ch2++ selects the cluster pairs which maximizes  $S_{Ch2++}$  for merging, until  $(c)$  clusters are left.

$$S_{Ch2++}(C_i, C_j) = R_{CL}(C_i, C_j)^\alpha \cdot R_{IC}(C_i, C_j), \quad (7)$$

Here,  $R_{CL}$  and  $R_{IC}$  are defined in (4) and (1). Further  $\alpha$  and  $\beta$  are user-defined parameters with default values of 2.0 and 1.0, respectively.

Algorithm	Graph Generation	Graph Partitioning	Partition Refinement	Merging
Ch2++	Approx. $k$ -NN ( <b>Annoy</b> )	hMETIS	Flood-Fill	$R_{CL}^\alpha * R_{IC}$
Complexity	$O(n \log n)$	$O(n + m \log m)$	$O(n)$	$O(m^2 \log m)$

**Table 8** Ch2++ at a glance.

With these modifications, the final complexity of Ch2++, as given in Table 8, is  $O(n \log n + n + m \log m + n + m^2 \log m)$ . Since  $(m \ll n)$ , the computational complexity of Ch2++ is bounded by  $O(n \log n)$ , surpassing that of Ch2.

## 3.2 Experimental Results

In this section, the dataset and evaluation metric are the same as used in section 2.3.1. Next, we initially give parametric configurations for our Ch2++ algorithm (in Section 3.2.1). Then, we do a run time analysis between our approximate  $k$ -NN and earlier exact  $k$ -NN (in Section 3.2.2). The approximate  $k$ -NN search algorithms, <sup>1</sup>Annoy, <sup>2</sup>FLANN and <sup>3</sup>NMSLIB are available in the form of libraries. Finally, we give performance results on Ch2++ and Ch2 (in Section 3.2.3). Since we have already demonstrated that hMETIS is computationally efficient than recursive FM bisection, all comparisons with Ch2 are conducted using the hMETIS-based implementation.

### 3.2.1 Parametric Configuration

Here, we give the parameter values for Ch2++ on the standard benchmark datasets. These values are categorized as default and fine-tuned for a each dataset. The default are given in Table 9 and the fine-tuned values are given in Table 10.

<sup>1</sup><https://github.com/spotify/annoy>

<sup>2</sup><https://github.com/flann-lib/flann>

<sup>3</sup><https://github.com/nmslib/nmslib>

Algorithm	Parameter	Description	Default Value
underlying Chameleon clustering	$m$	no. of partitions	$\max\{k, 2\text{classes}\}$
	$m_{fact}$	factor for small clusters	$10^3$
	$\alpha$	closeness	2.0
	$\beta$	interconnectivity	1.0
Annoy	$k$	no. of neighbors ( $k$ -NN)	$2 \log n$
	$t$	no. of trees	$2 \log n$
FLANN	$k$	no. of neighbors ( $k$ -NN)	$2 \log n$
	$t$	no. of trees	$2 \log n$
	$f$	indexing data-structure	$k$ -d tree
NMSLIB	$k$	no. of neighbors ( $k$ -NN)	$2 \log n$
	$M$	maximum neighbors	10
	$efC$	exploration factor	100
	$T$	threads	4

**Table 9** Default parameter values for the underlying Chameleon clustering, Chameleon2, Annoy, FLANN, NMSLIB.

Dataset	Annoy			FLANN				NMSLIB		
	$k$	$\alpha$	$\beta$	$k$	$t$	$\alpha$	$\beta$	$k$	$\alpha$	$\beta$
3-spiral	$\ln n$	-	-	4	4	-	-	4	-	-
aggregation	-	-	-	10	4	-	-	6	-	-
atom	-	-	-	-	-	-	-	-	-	-
chainlink	-	-	-	-	-	-	-	-	-	-
cluto-t4.8k	-	-	-	12	8	4.0	2.0	39	5.0	3.0
cluto-t5.8k	$3 \log 2n$	4.0	2.0	11	8	4.0	2.0	39	6.0	3.0
cluto-t7.10k	$3 \log 2n - 2$	2.0	3.0	14	12	-	3.0	12	-	3.0
cluto-t8.8k	$3 \log 2n$	2.0	3.0	20	12	-	3.0	39	-	3.0
compound	$2 \ln n$	-	-	10	8	-	-	8	-	-
cure-t2-4k	$\ln n$	-	-	19	12	-	-	7	-	-
D31	-	-	-	10	4	-	-	10	-	-
dense-disk-5k	$3 \log 2n + 3$	2.0	3.0	13	12	1.0	4.0	13	1.0	4.0
diamond9	$\log 2n$	-	-	10	8	-	-	12	-	-
disk-in-disk	$3 \log 2n + 2$	2.0	4.0	6	8	-	4.0	20	-	4.0
dpb	$\log 2n$	-	-	9	12	3.0	4.0	35	3.0	4.0
DS-850	$\log 2n$	-	-	12	4	-	-	14	-	-
flame	$\log 2n + 2$	-	-	12	8	-	-	12	-	-
impossible	$\ln n + 2$	2.0	3.0	12	6	-	-	9	-	-
jain	$2 \ln n$	-	-	6	4	-	-	6	-	-
long1	-	-	-	11	12	-	-	9	-	-
longsquare	-	-	-	6	4	-	-	5	-	-
lsun	$2 \ln n$	-	-	6	4	-	-	6	-	-
pathbased	-	-	-	9	8	-	-	7	-	-
s-set1	-	-	-	21	12	-	-	19	-	-
sizes1	$\log 2n$	-	-	11	8	-	-	6	-	-
smile1	-	-	-	9	12	-	-	10	-	-
spiralsquare	-	-	-	11	8	-	-	14	-	-
target	$2 \ln n$	-	-	9	4	-	-	9	-	-
triangle1	-	-	-	7	8	-	-	7	-	-
twodiamonds	-	-	-	7	8	-	-	6	-	-
wingnut	-	-	-	5	12	-	-	5	-	-
zelnik4	-	-	-	6	12	-	-	6	-	-

**Table 10** Fine-tuned parameter values for Ch2++.

### 3.2.2 Run Time Analysis: Exact $k$ -NN v/s Approx. $k$ -NN

Dataset	$n$	$k$ -NN (s)	Annoy (s)	Gain (%)
flame	240	0.424	0.016	96.23
pathbased	300	0.665	0.026	96.09
3-spiral	312	0.727	0.025	96.56
jain	373	0.994	0.031	96.88
compound	399	1.322	0.047	96.44
lsun	400	1.148	0.037	96.78
zelnik4	622	2.836	0.067	97.64
target	770	4.315	0.124	97.13
aggregation	788	4.382	0.077	98.24
atom	800	4.585	0.093	97.97
twodiamonds	800	4.585	0.083	98.19
DS-850	850	5.128	0.119	97.68
longsquare	900	5.967	0.097	98.37
chainlink	1,000	7.656	0.113	98.52
smile1	1,000	7.090	0.110	98.45
triangle1	1,000	7.161	0.109	98.48
long1	1,000	7.059	0.107	98.48
sizes1	1,000	7.368	0.111	98.49
wingnut	1,016	7.691	0.109	98.58
spiralsquare	1,500	15.88	0.196	98.77
disk-in-disk	3,000	65.26	0.469	99.28
diamond9	3,000	65.23	0.764	98.83
D31	3,100	68.56	0.441	99.36
impossible	3,673	96.89	0.691	99.29
dpb	4,000	113.54	0.588	99.48
cure-t2-4k	4,200	127.44	0.715	99.44
dense-disk-5k	5,000	178.62	0.945	99.47
s-set1	5,000	183.73	0.820	99.55
cluto-t5-8k	8,000	464.57	1.521	99.67
cluto-t4-8k	8,000	455.79	1.642	99.64
cluto-t8-8k	8,000	457.71	1.566	99.66
cluto-t7-10k	10,000	717.40	2.199	99.69

**Table 11** Runtime comparison between  $k$ -NN and Annoy.

As discussed earlier, we theoretically know that the computational complexity of approximate  $k$ -NN algorithm is lower than that of exact  $k$ -NN, i.e.,  $O(n \log n)$  instead of  $O(n^2)$ , where  $n$  is the data size. Here, we experimentally demonstrate that approximate  $k$ -NN based graph generation (and especially Annoy which performs best among available choices) has lower runtime than exact  $k$ -NN. The results for this are given in Table 11.



This table consists of five columns: Column 1 lists the standard benchmark datasets, Column 2 indicates the size of each dataset ( $n$ ), Columns 3 and 4 provide the runtime values for graph generation using  $k$ -NN and Annoy, respectively, and Column 5 lists the percentage throughput gain achieved by Annoy over  $k$ -NN. The corresponding data is plotted in Fig. 14.

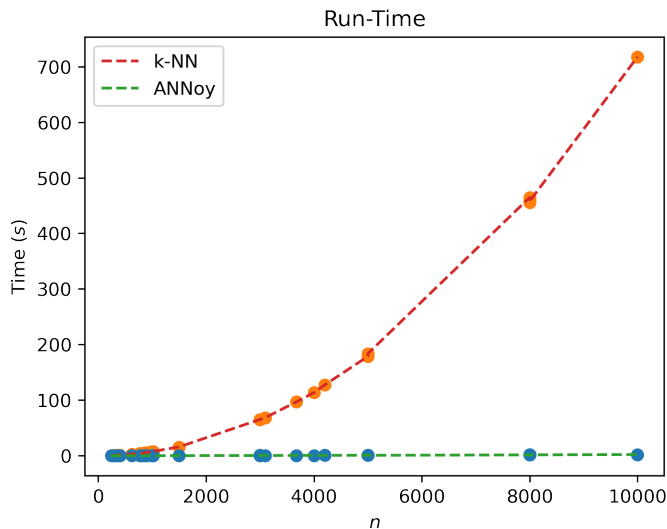


**Fig. 14** Annoy outperforms  $k$ -NN.

The results clearly demonstrates that Annoy consistently outperforms the conventional  $k$ -NN algorithm across all datasets, with an average performance gain exceeding 98.3%. These findings underscore the superior runtime efficiency of Annoy over  $k$ -NN.

### 3.2.3 Results

Here in Table 12, we present NMI values when using different approximate nearest neighbor search algorithms in Ch2++, and as well as Ch2. Column 1 lists the dataset. Column 2, 3, and 4 give the NMI values for Ch2++ when using Annoy, FLANN, and NMSLIB, respectively. Finally, column 5 presents the NMI values for Ch2. Here, the best value for a dataset is highlighted in bold.

Dataset	Ch2++			Ch2
	Annoy	FLANN	NMSLIB	
3-spiral	<b>1.00</b>	<b>1.00</b>	<b>1.00</b>	<b>1.00</b>
aggregation	0.97	<b>1.00</b>	0.99	0.97
atom	<b>1.00</b>	0.99	0.99	<b>1.00</b>
chainlink	<b>1.00</b>	<b>1.00</b>	<b>1.00</b>	<b>1.00</b>
cluto-t4.8k	<b>0.87</b>	0.82	0.82	0.82
cluto-t5.8k	0.82	0.81	0.82	<b>0.83</b>
cluto-t7.10k	<b>0.84</b>	0.65	<b>0.84</b>	0.77
cluto-t8.8k	0.87	0.80	0.81	<b>0.90</b>
compound	<b>0.98</b>	0.93	0.95	<b>0.98</b>
cure-t2-4k	<b>0.94</b>	0.82	0.91	0.92
D31	0.94	0.92	0.92	<b>0.95</b>
dense-disk-5k	0.77	0.67	0.78	<b>0.82</b>
diamond9	<b>1.00</b>	<b>1.00</b>	0.99	<b>1.00</b>
disk-in-disk	0.85	0.63	<b>0.87</b>	0.75
dpb	<b>0.77</b>	0.69	0.65	0.72
DS-850	0.98	0.96	0.98	<b>0.99</b>
flame	0.91	0.93	0.93	<b>0.96</b>
impossible	0.94	0.87	0.92	<b>0.96</b>
jain	0.99	<b>1.00</b>	<b>1.00</b>	<b>1.00</b>
long1	<b>1.00</b>	<b>1.00</b>	<b>1.00</b>	<b>1.00</b>
longsquare	0.95	0.83	0.84	<b>1.00</b>
lsun	<b>1.00</b>	<b>1.00</b>	<b>1.00</b>	<b>1.00</b>
pathbased	0.92	0.91	<b>0.99</b>	0.88
s-set1	0.96	<b>1.00</b>	0.90	0.98
sizes1	0.87	<b>0.92</b>	0.90	0.89
smile1	<b>1.00</b>	0.95	0.90	<b>1.00</b>
spiralsquare	<b>0.98</b>	0.91	0.91	0.97
target	<b>1.00</b>	0.97	<b>1.00</b>	<b>1.00</b>
triangle1	<b>1.00</b>	0.95	<b>1.00</b>	<b>1.00</b>
twodiamonds	<b>1.00</b>	<b>1.00</b>	<b>1.00</b>	<b>1.00</b>
wingnut	<b>1.00</b>	<b>1.00</b>	<b>1.00</b>	<b>1.00</b>
zelnik4	<b>0.99</b>	0.83	0.84	<b>0.99</b>
AVG. ( $\mu$ )	<b>0.94</b>	0.90	0.92	<b>0.94</b>
SD. ( $\sigma$ )	<b>0.07</b>	0.11	0.09	<b>0.07</b>

**Table 12** NMI values for clustering results generated by Ch2++ using approximate nearest neighbor search algorithms and Ch2 algorithms, respectively.

There are two insights here, first, Annoy consistently outperforms both FLANN and NMSLIB on all the datasets. Second, Annoy based Ch2 (i.e., Ch2++) has almost the same NMI values as that of Ch2. This is remarkable because this shows that the use of approximate  $k$ -NN (as in Ch2++) instead of exact  $k$ -NN (as in Ch2) leads to no loss in performance. On the contrary, Ch2++ has a lower computational complexity than Ch2. That is  $O(n \log n)$  instead of  $O(n^2)$ , where  $n$  is the size of dataset.

## 4 Conclusion and Future Work

Clustering is a vital unsupervised data analysis technique that groups data points to maximize intra-cluster similarity and minimize inter-cluster similarity, enabling the discovery of meaningful patterns in large datasets. Among clustering algorithms, Chameleon is a widely adopted hierarchical clustering method. However, while Ch2 significantly outperforms its predecessor (Ch1) and other competing algorithms, it has notable shortcomings that we have effectively addressed and improved upon in this work.

Here in this thesis, we have addressed two failings of the Ch2 algorithm. First, we have showed that the computational complexity of the algorithm in practice turned out to be  $O(n^2 \log n)$ , as compared to the  $O(n^2)$  claimed by the original paper, where  $n$  is the number of data points. Second, we have meticulously provided fine-tuned parameters for Ch2 to enhance replicability and promote transparency.

We have improved Ch2 by replacing exact  $k$ -NN search by an approximate one. This has resulted in reducing its computational complexity down to  $O(n \log n)$  with no performance loss.

There are multiple future directions here, one involves applying these techniques to other clustering algorithms like spectral clustering (Shastri et al. 2019). Second interesting direction would be to involve compressed sensing in this domain (Agrawal and Ahuja 2021). Third direction would be to work out the numerical analysis underlying this algorithm (Choudhary and Ahuja 2018). Last suggested direction would be to apply the new Chameleon2++ algorithm in complex information systems (Kim et al. 2005).

## References

- [1] Xu, D., Tian, Y.: A comprehensive survey of clustering algorithms. *Annals of Data Science* **2**, 165–193 (2015)
- [2] Karypis, G., Han, E.-H., Kumar, V.: Chameleon: Hierarchical clustering using dynamic modeling. *Computer* **32**(8), 68–75 (1999)
- [3] Ezugwu, A.E., Ikotun, A.M., Oyelade, O.O., Abualigah, L., Agushaka, J.O., Eke, C.I., Akinyelu, A.A.: A comprehensive survey of clustering algorithms: State-of-the-art machine learning applications, taxonomy, challenges, and future research prospects. *Engineering Applications of Artificial Intelligence* **110**, 104743 (2022)
- [4] Barton, T., Bruna, T., Kordik, P.: Chameleon 2: An improved graph-based clustering algorithm. *ACM Transactions on Knowledge Discovery from Data (TKDD)* **13**(1), 1–27 (2019)
- [5] Taunk, K., De, S., Verma, S., Swetapadma, A.: A brief review of nearest neighbor

- algorithm for learning and classification. In: Proceedings of International Conference on Intelligent Computing and Control Systems (ICCS), pp. 1255–1260 (2019). IEEE
- [6] Kernighan, B.W., Lin, S.: An efficient heuristic procedure for partitioning graphs. *The Bell System Technical Journal* **49**(2), 291–307 (1970)
- [7] Karypis, G., Aggarwal, R., Kumar, V., Shekhar, S.: Multilevel hypergraph partitioning: Application in vlsi domain. In: Proceedings of the 34th Annual Design Automation Conference, pp. 526–529 (1997)
- [8] Schlag, S., Heuer, T., Gottesbüren, L., Akhremtsev, Y., Schulz, C., Sanders, P.: High-quality hypergraph partitioning. *ACM Journal of Experimental Algorithmics* **27**, 1–39 (2023)
- [9] Karypis, G., Kumar, V.: A hypergraph partitioning package. Army HPC Research Center, Department of Computer Science & Engineering, University of Minnesota (1998)
- [10] Karypis, G., Kumar, V.: Multilevel k-way hypergraph partitioning. In: Proceedings of the 36th Annual ACM/IEEE Design Automation Conference, pp. 343–348 (1999)
- [11] Saxena, A., Prasad, M., Gupta, A., Bharill, N., Patel, O.P., Tiwari, A., Er, M.J., Ding, W., Lin, C.-T.: A review of clustering techniques and developments. *Neurocomputing* **267**, 664–681 (2017)
- [12] Shatovska, T., Onoprienko, O., Fedorov, A.: A modified multilevel approach to the dynamic hierarchical clustering for complex types of shapes. *Eastern-European Journal of Enterprise Technologies* **2**(11 (56)), 11–14 (2012)
- [13] Shannon, C.E.: A mathematical theory of communication. *The Bell System Technical Journal* **27**(3), 379–423 (1948)
- [14] Abbasifard, M.R., Ghahremani, B., Naderi, H.: A survey on nearest neighbor search methods. *International Journal of Computer Applications* **95**(25) (2014)
- [15] Li, W., Zhang, Y., Sun, Y., Wang, W., Li, M., Zhang, W., Lin, X.: Approximate nearest neighbor search on high dimensional data—experiments, analyses, and improvement. *IEEE Transactions on Knowledge and Data Engineering* **32**(8), 1475–1488 (2019)
- [16] Aumüller, M., Bernhardsson, E., Faithfull, A.: Ann-benchmarks: A benchmarking tool for approximate nearest neighbor algorithms. *Information Systems* **87**, 101374 (2020)
- [17] Malkov, Y., Ponomarenko, A., Logvinov, A., Krylov, V.: Approximate nearest

- neighbor algorithm based on navigable small world graphs. *Information Systems* **45**, 61–68 (2014)
- [18] Dasgupta, S., Freund, Y.: Random projection trees and low dimensional manifolds. In: *Proceedings of the 40th Annual ACM Symposium on Theory of Computing*, pp. 537–546 (2008)
- [19] Otair, D.M.: Approximate k-nearest neighbour based spatial clustering using kd tree. arXiv preprint arXiv:1303.1951 (2013)
- [20] Malkov, Y.A., Yashunin, D.A.: Efficient and robust approximate nearest neighbor search using hierarchical navigable small world graphs. *IEEE Transactions on Pattern Analysis and Machine Intelligence* **42**(4), 824–836 (2018)
- [21] Shastri, A.A., Ahuja, K., Ratnaparkhe, M.B., Shah, A., Gagrani, A., Lal, A.: Vector quantized Spectral Clustering applied to whole genome sequences of plants. *Evolutionary Bioinformatics* **15**, 1176934319836997 (2019)
- [22] Agrawal, R., Ahuja, K.: CSIS: Compressed sensing-based enhanced-embedding capacity image Steganography scheme. *IET Image Processing* **15**(9), 1909–1925 (2021)
- [23] Choudhary, R., Ahuja, K.: Stability analysis of bilinear iterative rational Krylov algorithm. *Linear Algebra and its Applications* **538**, 56–88 (2018)
- [24] Kim, S., Murthy, U., Ahuja, K., Vasile, S., Fox, E.A.: Effectiveness of implicit rating data on characterizing users in complex information systems. In: Rauber, A and Christodoulakis, S and Tjoa, A M (eds), *Research and Advanced Technology for Digital Libraries (ECDL 2005)*, Lecture Notes in Computer Science vol. 3652, pp. 186–194 (2005)